Coexistence of antiferromagnetic ordering and superconductivity in the $Ba(Fe_{0.961}Rh_{0.039})_2As_2$ compound studied by Mössbauer spectroscopy

P. Wang,[1] Z. M. Stadnik,[1,*] J. Żukrowski,[2] A. Thaler,[3] S. L. Bud'ko,[3] and P. C. Canfield[3]

[1]*Department of Physics, University of Ottawa, Ottawa, Ontario K1N 6N5, Canada*

[2]*Solid State Physics Department, Faculty of Physics and Applied Computer Science, AGH University of Science and Technology, PL-30-059 Kraków, Poland*

[3]*Ames Laboratory, US Department of Energy, and Department of Physics and Astronomy, Iowa State University, Ames, Iowa 50011, USA*

(Received 21 April 2011; revised manuscript received 20 May 2011; published 8 July 2011)

The results of a ^{57}Fe Mössbauer spectroscopy study between 2.0 and 294 K of superconducting $Ba(Fe_{0.961}Rh_{0.039})_2As_2$ are reported. The main component of the electric field gradient tensor at 294 K is shown to be positive and its increase with decreasing temperature is well described by a $T^{3/2}$ power-law relation. The shape of the Mössbauer spectra below the Néel temperature $T_N = 55.5(1)$ K is shown to result from the presence of doping-induced disorder rather than of incommensurate spin-density-wave order. The measured hyperfine magnetic field reaches its maximum value at the critical temperature $T_c = 14$ K and then decreases by 4.2% upon further cooling to 2.0 K. This constitutes direct evidence of the coexistence of and competition between superconductivity and magnetic order. The extrapolated value of the Fe magnetic moment at 0 K is determined to be 0.35(1) μ_B. The Debye temperature of $Ba(Fe_{0.961}Rh_{0.039})_2As_2$ is found to be 357(3) K.

DOI: 10.1103/PhysRevB.84.024509 PACS number(s): 74.70.−b, 76.80.+y

I. INTRODUCTION

The recent discovery of superconductivity in iron-pnictide compounds[1,2] has triggered intense research into its nature and origin. It has renewed interest in the relationship between antiferromagnetism found in these superconductors and superconductivity.[3] In particular, the possibility of incommensurability of the antiferromagnetic order is still an unsettled issue for the *R*OFeAs (*R* = rare earth) and AFe_2As_2 (*A* = Ba, Sr, Ca, K) superconductors.

On the theoretical side, various theoretical models suggest the coexistence of superconductivity and incommensurate antiferromagnetic order in doped *R*OFeAs and AFe_2As_2 superconductors.[4] Density-functional theory calculations[5] invoke incommensurability to explain the anisotropy of the spin excitation spectrum of the $Ba(Fe_{0.926}Co_{0.074})_2As_2$ superconductor.[6] On the experimental side, neutron-diffraction experiments did not detect any incommensurability within their resolution window.[7] Also, x-ray resonant magnetic diffraction measurements of the $Ba(Fe_{0.953}Co_{0.047})_2As_2$ superconductor[8] and ^{75}As NMR measurements of the $Ba(Fe_{1-x}Ni_x)_2As_2$ superconductors[9] found no evidence of incommensurability. On the other hand, muon spin relaxation experiments of the $LaFeAsO_{0.97}F_{0.03}$ superconductor,[10] ^{75}As and ^{59}Co NMR measurements of the $Ba(Fe_{1-x}Co_x)_2As_2$ superconductors,[11,12] and ^{57}Fe Mössbauer spectroscopy (MS) measurements of the $Ba(Fe_{1-x}Co_x)_2As_2$ (Ref. 13), $Ba(Fe_{1-x}Ni_x)_2As_2$ (Ref. 14), and $EuFe_2(As_{1-x}P_x)_2$ (Ref. 15) superconductors, and of the parent compounds AFe_2As_2 (A = Ca, Ba, Eu),[16] were all interpreted in terms of incommensurate spin-density-wave (SDW) order. Also, recent muon spin rotation and infrared spectroscopy experiments on $BaFe_{1.89}Co_{0.11}As_2$ suggested incommensurate SDW order.[17] Very recently, well-defined incommensurate spin fluctuations have been observed in the hole-overdoped KFe_2As_2 superconductor.[18]

The MS technique is, in principle, a valuable tool for study of the possibilities of incommensurate magnetic order in a given compound. This is because incommensurability results in an unusual shape of the Mössbauer spectra.[19,20] Here we use ^{57}Fe MS to identify the nature of antiferromagnetic ordering in the $Ba(Fe_{0.961}Rh_{0.039})_2As_2$ superconductor. We show that the shape of the high-quality ^{57}Fe Mössbauer spectra at temperatures below T_N is more likely to result from doping-induced disorder than from incommensuarate SDW order. We also observe, for the first time with the MS technique, a 4.2% reduction in the hyperfine magnetic field on cooling through the critical temperature T_c.

II. EXPERIMENTAL METHODS

Single crystals of $Ba(Fe_{0.961}Rh_{0.039})_2As_2$ used in this study were grown from an FeAs self-flux using a standard high-temperature-solution growth technique.[21] The chemical composition of the crystals was determined by using wavelength dispersive x-ray spectroscopy.[21]

Structural, magnetic, and transport properties of $Ba(Fe_{0.961}Rh_{0.039})_2As_2$ were determined from x-ray and neutron diffraction, magnetization, and electrical resistivity measurements.[21,22] $Ba(Fe_{0.961}Rh_{0.039})_2As_2$ crystallizes in a tetragonal $ThCr_2Si_2$-type crystal structure [space group $I4/mmm$ (No. 139)] and undergoes a structural phase transition to an orthorhombic crystal structure [space group $Fmmm$ (No. 69)] at $T_S = 59$ K.[22] The compound studied is a superconductor with $T_c = 14$ K and orders antiferromagnetically at $T_N = 54$ K.[22]

^{57}Fe Mössbauer measurements were conducted using a standard Mössbauer spectrometer operating in sine mode and a ^{57}Co(Rh) source at room temperature. The spectrometer was calibrated with a 6.35-μm-thick α-Fe foil[23] and the spectra were folded. As-grown crystals of $Ba(Fe_{0.961}Rh_{0.039})_2As_2$ are in the form of plates, with the tetragonal *c*-axis perpendicular to the plate. They could easily be cleaved, using a scalpel, into many flat plates of ∼50-μm thickness. The Mössbauer absorber was made from several such plates by attaching

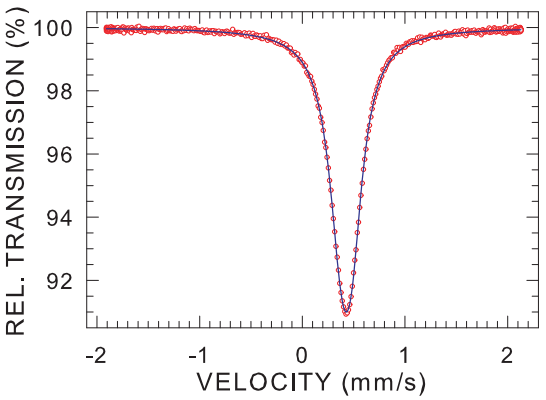

FIG. 1. (Color online) ^{57}Fe Mössbauer spectrum of $Ba(Fe_{0.961}Rh_{0.039})_2As_2$ at 294.3 K fitted (solid line) with an asymmetric quadrupole doublet, as described in the text. The zero-velocity origin is relative to α-Fe at room temperature.

them with Apiezon N grease to a high-purity, 8-μm-thick Al disk container to ensure a uniform temperature over the whole absorber. The plates overlapped slightly to avoid gaps between them. The direction of the γ rays was perpendicular to the surface of the plates, that is, parallel to the c axis. The Mössbauer absorber thickness of 50 μm corresponds to an effective thickness parameter[24] $T = 5.1 f_a$, where f_a is the Lamb-Mössbauer factor of the absorber. Since $T > 1$, the resonance line shape of the Mössbauer spectrum was described using a transmission integral formula.[25] The source line width $\Gamma_s = 0.107$ mm/s and the background-corrected Debye-Waller factor of the source f_s^*,[25] which were derived from the fit of the Mössbauer spectrum of the Fe foil, were used. As the electric quadrupole interaction is significantly smaller than the magnetic dipole interaction in the compound studied, the ^{57}Fe Zeeman spectra at temperatures below T_N were analyzed using a first-order perturbation treatment.[24]

III. EXPERIMENTAL RESULTS AND DISCUSSION

The ^{57}Fe Mössbauer spectrum of $Ba(Fe_{0.961}Rh_{0.039})_2As_2$ at room temperature, that is, far above T_N, is shown in Fig. 1. It has the appearance of a single narrow line. The Fe atoms in the studied compound are located at the 4d site (tetragonal

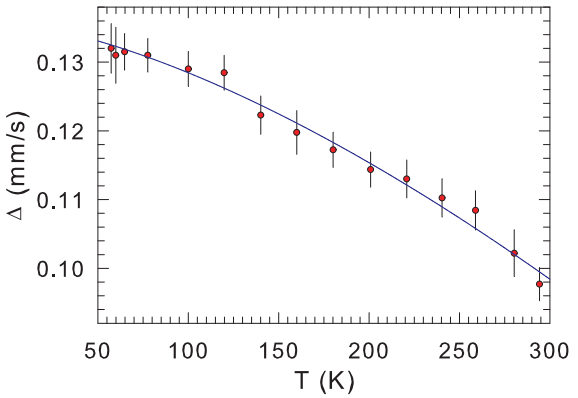

FIG. 2. (Color online) Temperature dependence of the quadrupole splitting Δ of $Ba(Fe_{0.961}Rh_{0.039})_2As_2$. The solid line is the fit to Eq. (1).

space group $I4/mmm$) with the point symmetry $\bar{4}m2$, which ensures an axially symmetric (the asymmetry parameter $\eta = 0$), nonzero electric field gradient (EFG) tensor at that site and, hence, a nonzero electric quadrupole hyperfine interaction.[24] The spectrum in Fig. 1 was fitted with an asymmetric quadrupole doublet and the intensity ratio of the higher-energy line to the lower-energy line of the doublet obtained from the fit was close to 3:1. As the $\bar{4}m2$ point symmetry of the Fe(4d) site requires that the principal axis of the EFG tensor lie along the crystallographic c axis, the intensity ratio 3:1 of the component lines of the doublet indicates that the principal component of the EFG tensor V_{zz} is positive.[24] The values of the absorber line width Γ_a, the quadrupole splitting $\Delta = \frac{1}{2} e Q V_{zz}$, where e is the proton charge and Q is the electric quadrupole moment of the ^{57}Fe nucleus,[26] and the center shift δ (relative to α-Fe at 298 K) obtained from the fit are, respectively, 0.098(2), 0.121(3), and 0.431(5) mm/s. The Δ value of 0.098(2) mm/s implies that $V_{zz} = 6.26(15) \times 10^{20}$ V/m^2. The value of Δ is, within experimental error, the same as that of 0.092(4) mm/s for the parent compound $BaFe_2As_2$.[14]

Fourteen ^{57}Fe Mössbauer spectra of $Ba(Fe_{0.961}Rh_{0.039})_2As_2$ (not shown here) recorded at temperatures between 280.3 and 57.3 K, at which no magnetic dipole hyperfine interaction[24] is present, are very similar to the spectrum shown in Fig. 1. They

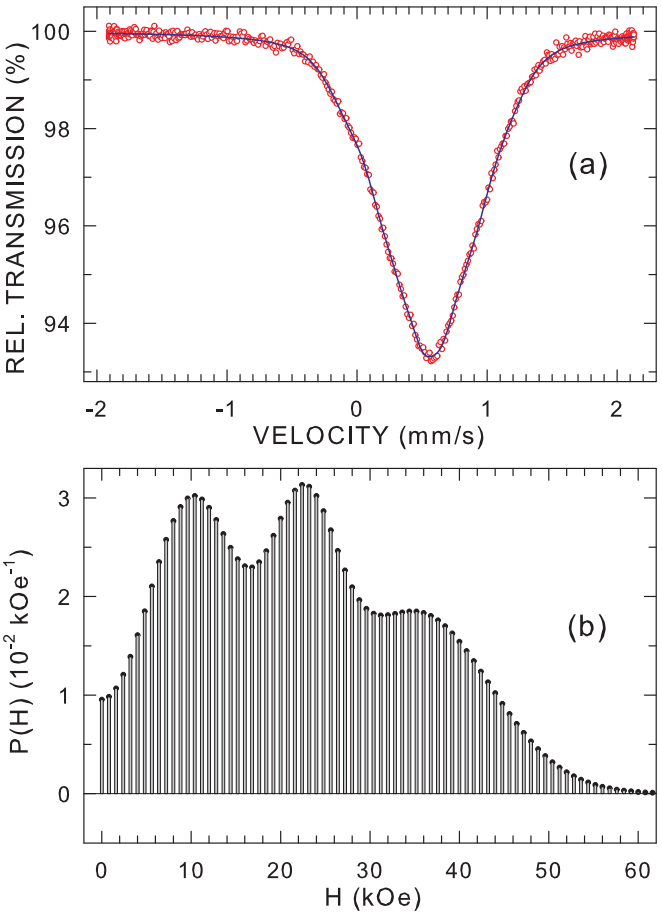

FIG. 3. (Color online) (a) ^{57}Fe Mössbauer spectrum of $Ba(Fe_{0.961}Rh_{0.039})_2As_2$ at 2.0 K fitted (solid line) with the disorder-induced hyperfine magnetic field distribution $P(H)$ shown in (b).

were fitted with an asymmetric quadrupole doublet pattern. The values of Δ derived from the fits of these spectra and of the spectrum in Fig. 1 are shown in Fig. 2. One can observe a clear increase in Δ with decreasing temperature (Fig. 2). Such a temperature dependence of Δ is found in many noncubic metallic systems[27] and is well described by the empirical equation

$$\Delta(T) = \Delta(0)(1 - BT^{3/2}), \quad (1)$$

where $\Delta(0)$ is the value of Δ at 0 K and B is a constant. The fit of the $\Delta(T)$ data (Fig. 2) to Eq. (1) gives $\Delta(0) = 0.136(1)$ mm/s and $B = 5.28(16) \times 10^{-5}$ K$^{-3/2}$. The value of B is similar to that found for other metallic systems.[27]

The ^{57}Fe Mössbauer spectrum of $Ba(Fe_{0.961}Rh_{0.039})_2As_2$ at 2.0 K, that is, much below T_N, is shown in Fig. 3(a). The shape of this spectrum is completely different from the six-line Zeeman pattern expected for an antiferromagnetic

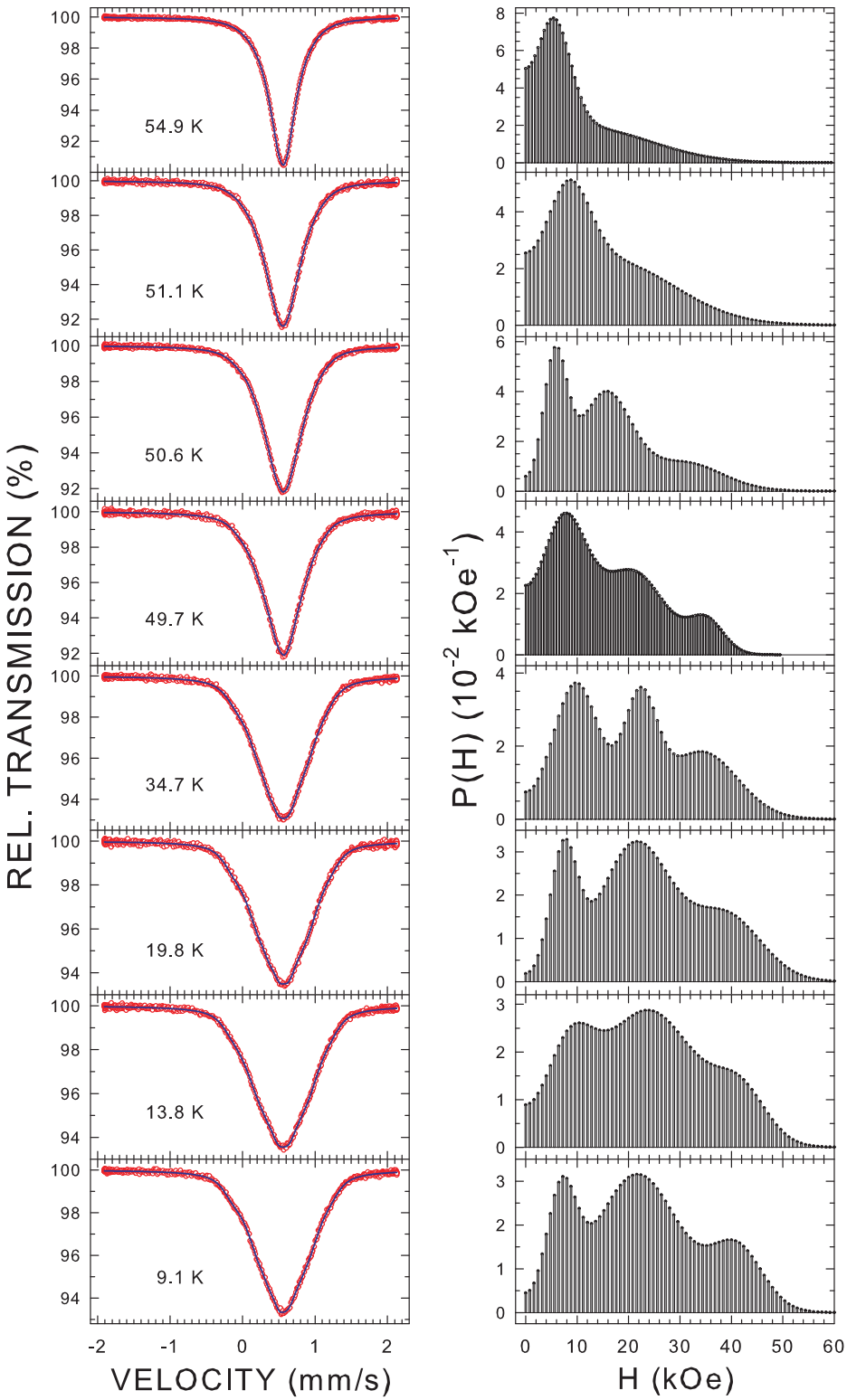

FIG. 4. (Color online) ^{57}Fe Mössbauer spectra of $Ba(Fe_{0.961}Rh_{0.039})_2As_2$ at the indicated temperatures (left panels) fitted (solid line) with the disorder-induced hyperfine magnetic field distribution $P(H)$ (right panels).

compound in which Fe atoms occupy one crystallographic site.[24] It must certainly result from the presence of a wide distribution $P(H)$ of hyperfine magnetic fields H. Such a wide distribution $P(H)$ can arise either from significant disorder induced by Rh doping or from the incommensurate modulation of the antiferromagnetic structure, that is, from the incommensurate SDW. We first assume that the distribution $P(H)$ is due to doping-induced disorder and determine its shape by fitting the Mössbauer spectrum in Fig. 3(a) with the constrained version[28] of the model-independent Hesse-Rübartsch method.[29] The same values of δ and the electric quadrupole shift[24] ε were assumed for the elementary sextets. The best fit ($\chi^2 = 0.86$) of the Mössbauer spectrum in Fig. 3(a) was obtained with the distribution $P(H)$ shown in Fig. 3(b). The parameters derived from the fit are $\delta = 0.564(5)$ mm/s and $\varepsilon = -0.018(2)$ mm/s, and the average value of the hyperfine magnetic field derived from the $P(H)$ distribution $\overline{H} = 22.4(1)$ kOe.

Selected ^{57}Fe Mössbauer spectra of $Ba(Fe_{0.961}Rh_{0.039})_2As_2$ measured at 16 temperatures in the temperature range 4.7–54.9 K, at which the magnetic dipole hyperfine interaction is present,[24] are displayed in Fig. 4. Excellent fits of these spectra ($\chi^2 \approx 0.9$) were obtained with the Hesse-Rübartsch method for the $P(H)$ distributions shown in Fig. 4. It is interesting to observe that the trimodal distribution $P(H)$ at low temperatures evolves into a bimodal $P(H)$ at higher temperatures. For a completely random doping-induced disorder one would expect a unimodal distribution $P(H)$. The observed trimodality/bimodality of $P(H)$ seems to indicate a not completely random dopant-induced disorder.

The values of $\overline{H}$ obtained from the determined distributions $P(H)$ at all temperatures are shown in Fig. 5. One can observe the expected increase in $\overline{H}$ with decreasing temperature down to T_c (inset in Fig. 5) and then its clear reduction below T_c. The value of $\overline{H}$ decreases from 23.4(1) kOe at 13.8 K to 22.1(1) kOe at 2.0 K, a 4.2% reduction. The value of $\overline{H}$ at 0 K, which was derived from the extrapolation of the $\overline{H}$ data in Fig. 5, is $\overline{H}(0) = 22.3(2)$ kOe. The occurrence of nonzero $\overline{H}$ values at and below T_c clearly demonstrates the coexistence of superconductivity and antiferromagnetic order in the $Ba(Fe_{0.961}Rh_{0.039})_2As_2$ superconductor.

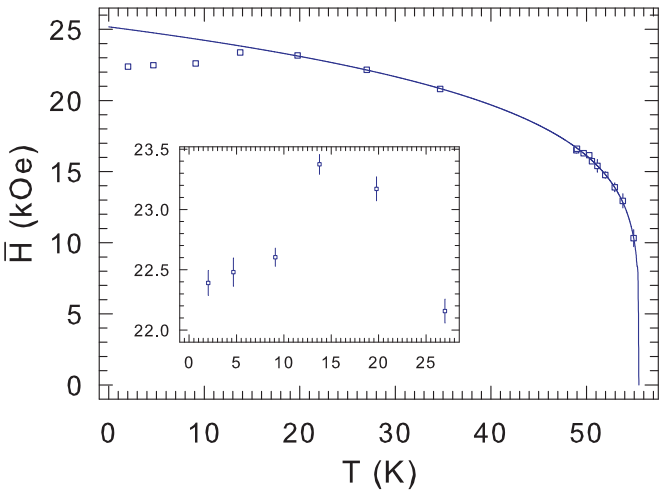

FIG. 5. (Color online) Temperature dependence of $\overline{H}$. Inset: An enlarged region around the superconducting transition T_c. The solid line is the power-law fit of the $\overline{H}$ data, as described in the text.

The measured H is, to a first approximation, proportional to μ_{Fe} through the relation $H = a\mu_{Fe}$, where the value of the proportionality constant a is compound specific.[24,30] In converting $\overline{H}$ to $\overline{\mu}_{Fe}$, we used $a = 63$ kOe/μ_B, which results from $H(4.2\text{ K}) = 54.7(1)$ kOe measured[31] for $BaFe_2As_2$ and $\mu_{Fe}(5\text{ K}) = 0.87(3)\mu_B$ determined from the neutron diffraction study of $BaFe_2As_2$.[32] Thus, $\overline{H}(0) = 22.3(2)$ kOe corresponds to $\overline{\mu}_{Fe}(0) = 0.35(1)\mu_B$, which is in good agreement with the value $\mu_{Fe}(0) = 0.37(10)\mu_B$ determined from the neutron diffraction study of $Ba(Fe_{0.961}Rh_{0.039})_2As_2$.[22] The observed reduction of $\overline{H}$, which is equivalent to the reduction of $\overline{\mu}_{Fe}$, upon cooling through T_c (Fig. 5), observed here for the first time using MS, constitutes clear evidence of the competition between superconductivity and the long-range antiferromagnetic order.

The $\overline{H}$ data (Fig. 5) could be fitted to the power law over the limited range of temperatures ($34.7\text{ K} \leqslant T \leqslant 54.9$ K). The fit yielded the the Néel temperature $T_N = 55.5(1)$ K, which

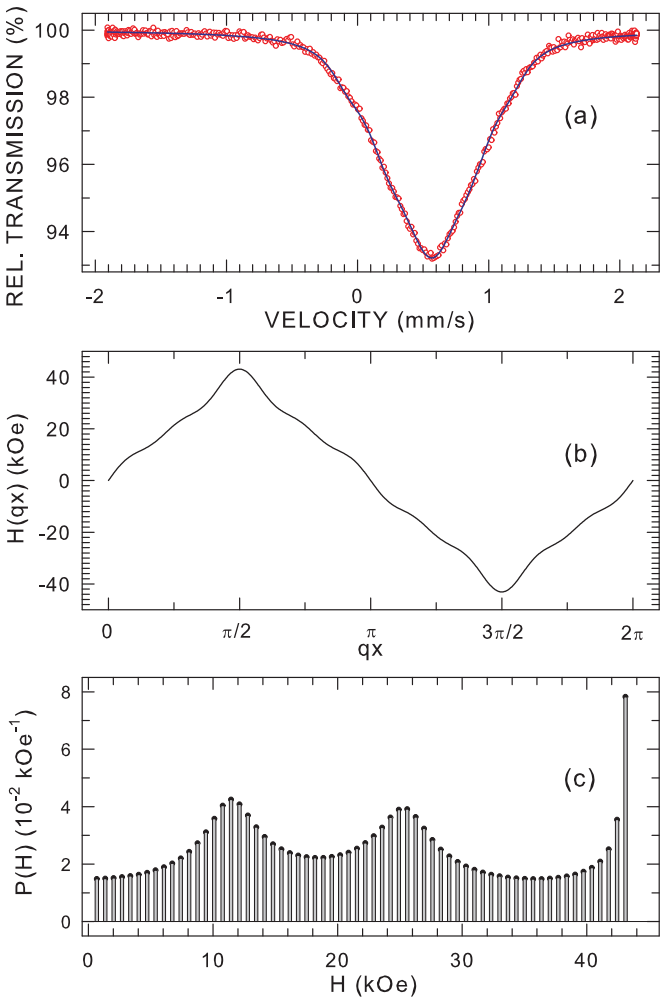

FIG. 6. (Color online) (a) ^{57}Fe Mössbauer spectrum of $Ba(Fe_{0.961}Rh_{0.039})_2As_2$ at 2.0 K fitted (solid line) with an incommensurate modulation of the hyperfine magnetic field, as described in the text. (b) Resulting shape of the spin density wave. (c) Resulting hyperfine magnetic field distribution.

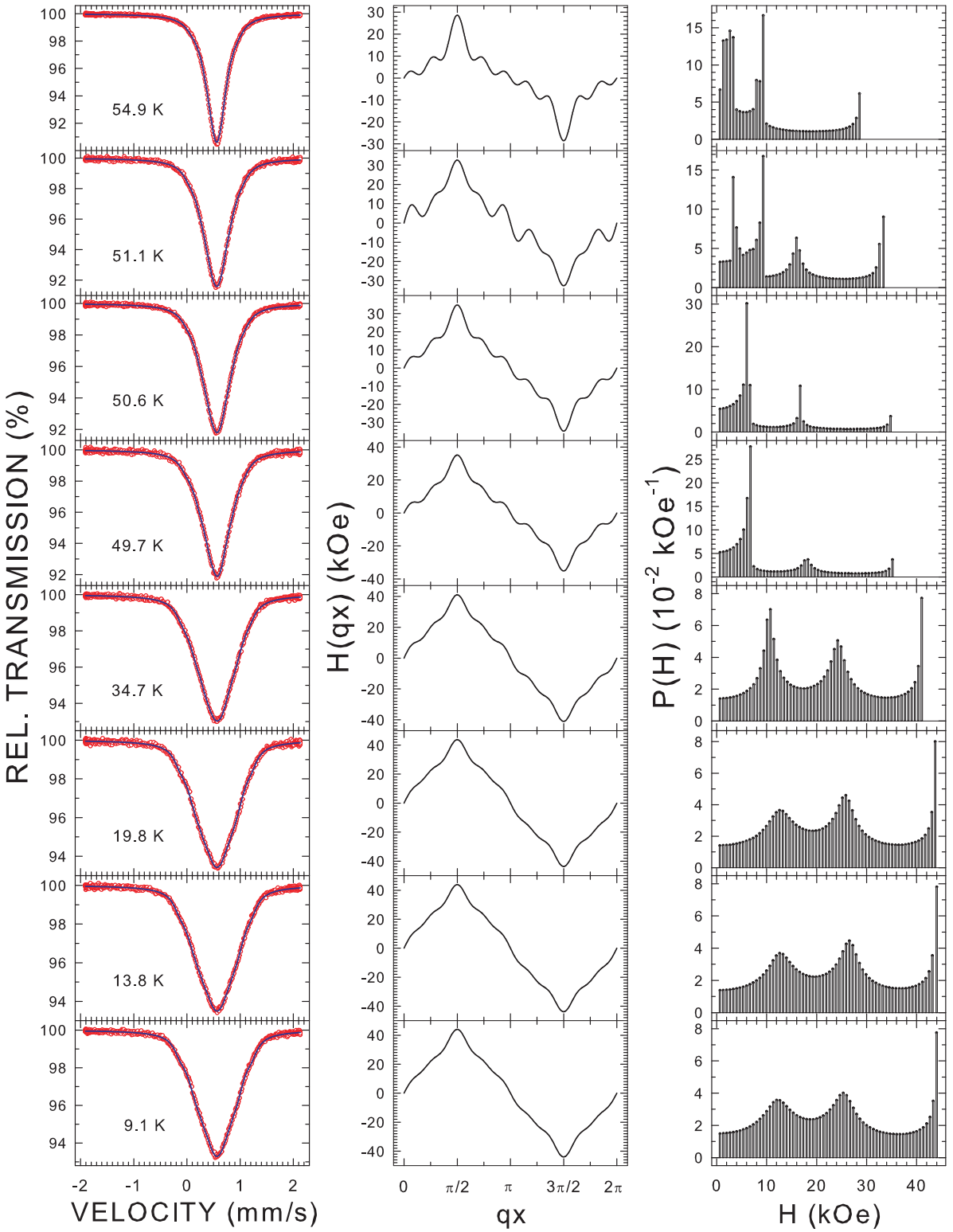

FIG. 7. (Color online) ^{57}Fe Mössbauer spectra of $Ba(Fe_{0.961}Rh_{0.039})_2As_2$ at the indicated temperatures fitted (solid line) with an incommensurate modulation of the hyperfine magnetic field (left panels), the corresponding shapes of the spin density wave (middle panels), and the resulting hyperfine magnetic field distributions (right panels).

is close to the value of 54 K determined from the neutron diffraction study.[22]

Let us now assume that the distribution $P(H)$ resulting in the 2.0 K Mössbauer spectrum shown in Fig. 6(a) is caused by the incommensurate SDW. Assuming a collinear antiferromagnetic structure (the Fe magnetic moments are aligned antiferromagnetically along the orthorhombic a axis)[22] and collinearity of the Fe magnetic moment and H, one can

describe the amplitude of the SDW (the hyperfine magnetic field H) along the x direction parallel to the wave vector $\mathbf{q}$ as a series of odd harmonics,[13,20]

$$H(qx) = \sum_{i=1}^{n} h_{2i-1} \sin[(2i-1)qx], \qquad (2)$$

where h_{2i-1} is the amplitude of the $(2i-1)$th harmonic, q is the wave number of the SDW, x is the relative position of the Fe atom along the direction of SDW propagation, and n denotes the maximum number of harmonics; the periodicity of the SDW demands that $0 \leqslant qx \leqslant 2\pi$. A Mössbauer spectrum is then fitted to a set of six-line Zeeman patterns corresponding to H values calculated from Eq. (2) for discrete qx values in the range $\langle 0, 2\pi \rangle$. We assume the same values of δ and ε for each Zeeman pattern. The resulting distribution $P(H)$ can then be calculated from the amplitudes h_{2i-1} determined from the fit. The average value of H given by Eq. (2) is obviously 0, and so the root-mean-square value of H can be obtained from the expression $H_{\rm rms} = \sqrt{\frac{1}{2}\sum_{i=1}^{n} h_{2i-1}^2}$.[13] The square of $H_{\rm rms}$ is proportional to the intensity of a magnetic Bragg peak in neutron diffraction.[13] Hence, $H_{\rm rms}$ is proportional to the magnetic moment $\mu_{\rm Fe}$ of the Fe atoms.

An excellent fit ($\chi^2 = 0.99$) of the Mössbauer spectrum in Fig. 6(a) could be achieved using $n = 5$ harmonics (*vide infra*), with the resulting shape of the SDW shown in Fig. 6(b) and the corresponding distribution $P(H)$ shown in Fig. 6(c). The parameters derived from the fit are $\delta = 0.569(6)$ mm/s and $\varepsilon = -0.021(3)$ mm/s, the maximum value of the hyperfine magnetic field $H_{\rm max} = 43.1(1)$ kOe, the average value of the hyperfine magnetic field derived from the $P(H)$ distribution $\overline{H} = 21.5(1)$ kOe, and $H_{\rm rms} = 24.6(2)$ kOe.

Very good fits ($\chi^2 \approx 1.1$) could be obtained also for the ^{57}Fe Mössbauer spectra recorded at other temperatures at which the magnetic dipole hyperfine interaction is present (Fig. 7) using $n = 5$ harmonics, and the resulting shape of the SDW and the distribution $P(H)$ are shown for each of these spectra (Fig. 7). The values of the harmonic amplitudes resulting from the fits of all the spectra are shown in Fig. 8. The amplitude of the first harmonic h_1 is an order of magnitude higher than the absolute values of the higher harmonic amplitudes. It increases slightly with increasing temperature in the temperature range 2–14 K and then decreases monotonically with increasing temperature. The temperature dependence of the amplitudes of higher harmonics h_3, h_5, h_7, and h_9 is smaller than that of h_1.

The temperature dependence of the three hyperfine magnetic fields $H_{\rm max}$, $\overline{H}$, and $H_{\rm rms}$ obtained from the fits of all the spectra is shown in Fig. 9. These three fields increase with decreasing temperature down to T_c (insets in Fig. 9) and then clearly decrease below T_c. The value of $H_{\rm rms}$ decreases from 25.5(2) kOe at 13.8 K to 24.6(2) kOe at 2.0 K, a 3.5% reduction. The value of $H_{\rm rms}$ at 0 K, which was derived from the extrapolation of the $H_{\rm rms}(T)$ data in Fig. 9, is $H_{\rm rms}(0) = 24.4(2)$ kOe, which corresponds to $\mu_{Fe}(0) = 0.39(2)\mu_B$. The fit of the $H_{\rm rms}(T)$ data (Fig. 9) to the power law yields $T_N = 55.4(5)$ K.

The two analyses presented above of the Mössbauer spectra recorded at temperatures at which the magnetic dipole hyperfine interaction occurs show that the fits of these spectra with the distribution $P(H)$ resulting from the dopant-induced disorder are only marginally better than the fits with the distribution $P(H)$ due to the incommensurate SDW. Thus, one cannot state conclusively that the Mössbauer spectra result from the presence of dopant-induced disorder rather than from the existence of incommensurate SDW. One notes, however, that the relevant physical parameters derived from these two analyses have very much the same values and temperature dependencies. The SDW incommensurability is most directly detected in neutron and x-ray resonant scattering experiments. These experiments clearly demonstrate the existence of commensurate antiferromagnetic order in the $Ba(Fe_{1-x}T_x)_2As_2$ (T = Co, Ni, Rh) superconductors.[7,8,22] It would thus appear that the analysis of the Mössbauer spectra of $Ba(Fe_{0.961}Rh_{0.039})_2As_2$ in terms of the $P(H)$ distribution resulting from the dopant-induced disorder is more justified than that in terms of the $P(H)$ distribution due to incommensurate SDW.

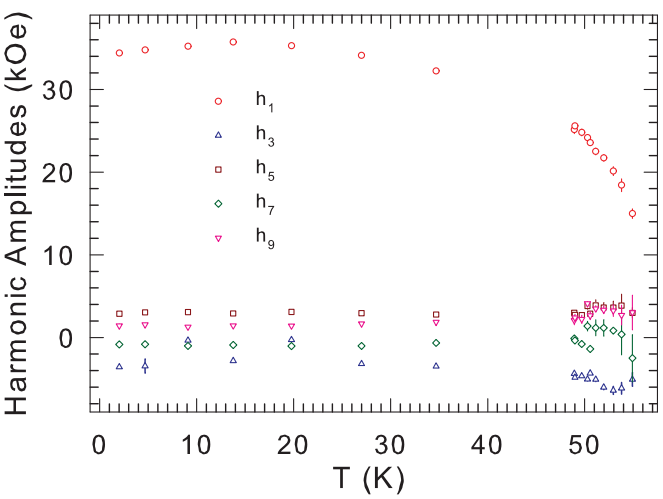

FIG. 8. (Color online) Temperature dependence of the harmonic amplitudes.

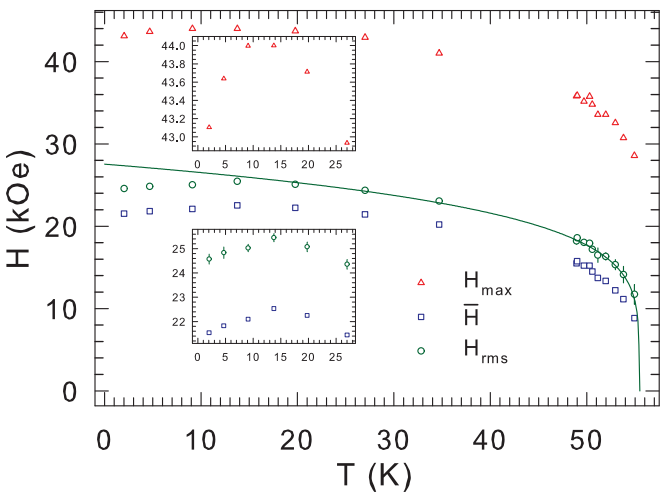

FIG. 9. (Color online) Temperature dependence of $H_{\rm max}$, $\overline{H}$, and $H_{\rm rms}$. Insets: An enlarged region around the superconducting transition T_c. The solid line is the power-law fit of the $H_{\rm rms}$ data, as described in the text.

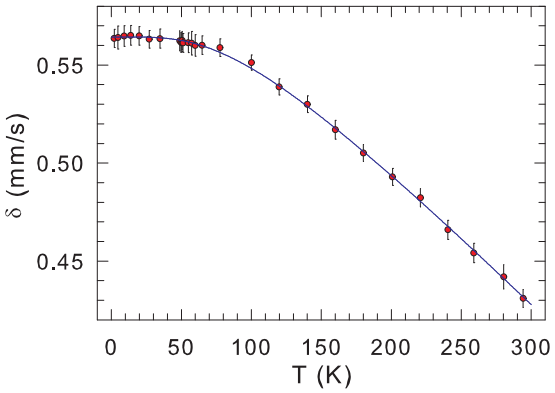

FIG. 10. (Color online) Temperature dependence of the center shift δ of $Ba(Fe_{0.961}Rh_{0.039})_2As_2$. The solid line is the fit to Eq. (3), as explained in the text.

The temperature dependence of $\delta(T)$, determined from the fits of the Mössbauer spectra measured at all temperatures, is shown in Fig. 10. $\delta(T)$ is given by

$$\delta(T) = \delta_0 + \delta_{\rm SOD}(T), \tag{3}$$

where δ_0 is the intrinsic isomer shift and $\delta_{\rm SOD}(T)$ is the second-order Doppler (SOD) shift, which depends on the lattice vibrations of the Fe atoms.[24] In terms of the Debye approximation of the lattice vibrations, $\delta_{\rm SOD}(T)$ is expressed[24] in terms of the Debye temperature Θ_D as

$$\delta_{\rm SOD}(T) = -\frac{9}{2}\frac{k_B T}{Mc}\left(\frac{T}{\Theta_D}\right)^3 \int_0^{\Theta_D/T} \frac{x^3 dx}{e^x - 1}, \tag{4}$$

where M is the mass of the Mössbauer nucleus and c is the speed of light. By fitting the experimental data to Eq. (3), the quantities δ_0 and Θ_D were found to be 0.564(1) mm/s and 357(3) K, respectively. The value of Θ_D found here is much larger than the reported Θ_D values of 134(1) K,[31] 186 K,[33] and 250 K[34] for $BaFe_2As_2$ derived from specific heat measurements. The most probable reason for this discrepancy is that a different weight of phonon frequency distribution is used in determining Θ_D from the specific heat data than from the Mössbauer data.[35]

IV. CONCLUSIONS

We report the results of ^{57}Fe MS measurements in the temperature range 2–294 K of the superconducting compound $Ba(Fe_{0.961}Rh_{0.039})_2As_2$. It is found that V_{zz} at 294 K is positive and that it increases with decreasing temperature according to a $T^{3/2}$ power-law relation. The unusual shape of the magnetically split Mössbauer spectra at temperatures between 2.0 K and $T_N = 55.5(1)$ K is interpreted in terms of the distribution of the hyperfine magnetic fields resulting from the dopant-induced disorder. The hyperfine magnetic field is found to reach a maximum at T_c and then to decrease upon further cooling down to 2.0 K. This is taken as evidence of competition between and the coexistence of magnetic order and superconductivity. The extrapolated magnetic moment of Fe atoms at 0 K is found to be 0.35(1) μ_B. The Debye temperature of $Ba(Fe_{0.961}Rh_{0.039})_2As_2$ is determined to be 357(3) K.

ACKNOWLEDGMENTS

This work was supported by the Natural Sciences and Engineering Research Council of Canada. Work at the Ames Laboratory was supported by the US Department of Energy, Office of Basic Energy Science, under Contract No. DE-AC02-07CH11358.

*stadnik@uottawa.ca

[1] Y. Kamihara, T. Watanabe, M. Hirano, and H. Hosono, J. Am. Chem. Soc. **130**, 3296 (2008).

[2] M. Rotter, M. Tegel, and D. Johrendt, Phys. Rev. Lett. **101**, 107006 (2008).

[3] M. D. Lumsden and A. D. Christianson, J. Phys. Condens. Matter **22**, 203203 (2010); J. Paglione and R. L. Greene, Nature Phys. **6**, 645 (2010); P. C. Canfield and S. L. Bud'ko, Annu. Rev. Condens. Matter Phys. **1**, 27 (2010); D. C. Johnston, Adv. Phys. **59**, 803 (2010); Y. Izyumov and E. Kurmaev, *High-T_c Superconductors Based on FeAs Compounds* (Springer, Berlin, 2010).

[4] A. B. Vorontsov, M. G. Vavilov, and A. V. Chubukov, Phys. Rev. B **79**, 060508(R) (2009); V. Cvetkovic and Z. Tesanovic, *ibid.* **80**, 024512 (2009); A. B. Vorontsov, M. G. Vavilov, and A. V. Chubukov, *ibid.* **81**, 174538 (2010); N. Lee and H.-Y. Choi, *ibid.* **82**, 174508 (2010).

[5] J. T. Park, D. S. Inosov, A. Yaresko, S. Graser, D. L. Sun, Ph. Bourges, Y. Sidis, Y. Li, J.-H. Kim, D. Haug, A. Ivanov, K. Hradil, A. Schneidewind, P. Link, E. Faulhaber, I. Glavatskyy, C. T. Lin, B. Keimer, and V. Hinkov, Phys. Rev. B **82**, 134503 (2010).

[6] H.-F. Li, C. Broholm, D. Vaknin, R. M. Fernandes, D. L. Abernathy, M. B. Stone, D. K. Pratt, W. Tian, Y. Qiu, N. Ni, S. O. Diallo, J. L. Zarestky, S. L. Bud'ko, P. C. Canfield, and R. J. McQueeney, Phys. Rev. B **82**, 140503 (2010).

[7] J. Zhao, Q. Huang, C. de la Cruz, S. Li, J. W. Lynn, Y. Chen, M. A. Green, G. F. Chen, G. Li, Z. Li, J. L. Luo, N. L. Wang, and P. Dai, Nat. Mater. **7**, 953 (2008); Y. Chen, J. W. Lynn, J. Li, G. Li, G. F. Chen, J. L. Luo, N. L. Wang, P. Dai, C. de la Cruz, and H. A. Mook, Phys. Rev. B **78**, 064515 (2008); J. Zhao, Q. Huang, C. de la Cruz, J. W. Lyn, M. D. Lumsden, Z. A. Ren, J. Yang, X. Shen, X. Dong, Z. Zhao, and P. Dai, *ibid.* **78**, 132504 (2008); C. Lester, J.-H. Cha, J. G. Analytis, S. C. Capelli, A. S. Erickson, C. L. Condron, M. F. Toney, I. R. Fisher, and S. M. Hayden, *ibid.* **79**, 144523 (2009); D. K. Pratt, W. Tian, A. Kreyssig, J. L. Zarestky, S. Nandi, N. Ni, S. L. Bud'ko, P. C. Canfield, A. I. Goldman, and R. J. McQueeney, Phys. Rev. Lett. **103**, 087001 (2009).

[8] M. G. Kim, A. Kreyssig, Y. B. Lee, J. W. Kim, D. K. Pratt, A. Thaler, S. L. Bud'ko, P. C. Canfield, B. N. Harmon, R. J. McQueeney, and A. I. Goldman, Phys. Rev. B **82**, 180412(R) (2010).

[9] A. P. Dioguardi, N. Roberts-Warren, A. C. Shockley, S. L. Bud'ko, N. Ni, P. C. Canfield, and N. J. Curro, Phys. Rev. B **82**, 140411(R) (2010).

[10] J. P. Carlo, Y. J. Uemura, T. Goko, G. J. MacDougall, J. A. Rodriguez, W. Yu, G. M. Luke, P. Dai, N. Shannon, S. Miyasaka, S. Suzuki, S. Tajima, G. F. Chen, W. Z. Hu, J. L. Luo, and N. L. Wang, Phys. Rev. Lett. **102**, 087001 (2009).

[11] Y. Laplace, J. Bobroff, F. Rullier-Albenque, D. Colson, and A. Forget, Phys. Rev. B **80**, 140501(R) (2009); Eur. Phys. J. B **73**, 161 (2010).

[12] F. Ning, K. Ahilan, T. Imai, A. S. Sefat, R. Jin, M. A. McGuire, B. C. Sales, and D. Mandrus, J. Phys. Soc. Jpn. **78**, 013711 (2009); F. L. Ning, K. Ahilan, T. Imai, A. S. Sefat, R. Jin, M. A. McGuire, B. C. Sales, and D. Mandrus, Phys. Rev. B **79**, 140506(R) (2009).

[13] P. Bonville, F. Rullier-Albenque, D. Colson, and A. Forget, Europhys. Lett. **89**, 67008 (2010).

[14] I. Nowik, I. Felner, N. Ni, S. L. Bud'ko, and P. C. Canfield, J. Phys. Condens. Matter **22**, 355701 (2010).

[15] I. Nowik, I. Felner, Z. Ren, G. H. Cao, and Z. A. Xu, J. Phys. Condens. Matter **23**, 065701 (2010).

[16] A. Błachowski, K. Ruebenbauer, J. Żukrowski, K. Rogacki, Z. Bukowski, and J. Karpinski, Phys. Rev. B **83**, 134410 (2011).

[17] P. Marsik, K. W. Kim, A. Dubroka, M. Rössle, V. K. Malik, L. Schulz, C. N. Wang, Ch. Niedermayer, A. J. Drew, M. Willis, T. Wolf, and C. Bernhard, Phys. Rev. Lett. **105**, 057001 (2010).

[18] C. H. Lee, K. Kihou, H. Kawano-Furukawa, T. Saito, A. Iyo, H. Eisaki, H. Fukazawa, Y. Kohori, K. Suzuki, H. Usui, K. Kuroki, and K. Yamada, Phys. Rev. Lett. **106**, 067003 (2011).

[19] R. Street, B. C. Munday, B. Window, and I. R. Williams, J. Appl. Phys. **39**, 1050 (1968).

[20] J. Cieślak and S. M. Dubiel, Nucl. Instrum. Methods Phys. Res., Sect. B **95**, 131 (1995), and references therein.

[21] N. Ni, A. Thaler, A. Kracher, J. Q. Yan, S. L. Bud'ko, and P. C. Canfield, Phys. Rev. B **80**, 024511 (2009).

[22] A. Kreyssig, M. G. Kim, S. Nandi, D. K. Prat, W. Tian, J. L. Zarestky, N. Ni, A. Thaler, S. L. Bud'ko, P. C. Canfield, R. J. McQueeney, and A. I. Goldman, Phys. Rev. B **81**, 134512 (2010).

[23] J. P. Cali, *Certificate of Calibration, Iron Foil Mössbauer Standard*, Natl. Bur. Stand. (US) Circ. No. 1541 (US Government Printing Office, Washington, DC, 1971).

[24] N. N. Greenwood and T. C. Gibb, *Mössbauer Spectroscopy* (Chapman and Hall, London, 1971); P. Gütlich, R. Link, and A. Trautwein, *Mössbauer Spectroscopy and Transition Metal Chemistry* (Springer, Berlin, 1978).

[25] S. Margulies and J. R. Ehrman, Nucl. Instrum. Methods **12**, 131 (1961); G. K. Shenoy, J. M. Friedt, H. Maletta, and S. L. Ruby, in *Mössbauer Effect Methodology*, edited by I. J. Gruverman, C. W. Seidel, and D. K. Dieterly (Plenum, New York, 1974), Vol. 10, p. 277.

[26] G. Martínez-Pinedo, P. Schwerdtfeger, E. Caurier, K. Langanke, W. Nazarewicz, and T. Söhnel, Phys. Rev. Lett. **87**, 062701 (2001).

[27] K. Al-Qadi, P. Wang, Z. M. Stadnik, and J. Przewoźnik, Phys. Rev. B **79**, 224202 (2009), and references therein.

[28] G. Le Caër and J. M. Dubois, J. Phys. E **12**, 1083 (1979).

[29] J. Hesse and A. Rübartsch, J. Phys. E **7**, 526 (1974).

[30] P. Panissod, J. Durand, and J. I. Budnik, Nucl. Instrum. Methods **199**, 99 (1982); P. Panissod, Hyperfine Interact. **24-26**, 607 (1985); O. Eriksson and A. Svane, J. Phys. Condens. Matter **1**, 1589 (1989); S. M. Dubiel, J. Alloys Compd. **488**, 18 (2009).

[31] M. Rotter, M. Tegel, D. Johrendt, I. Schellenberg, W. Hermes, and R. Pöttgen, Phys. Rev. B **78**, 020503(R) (2008).

[32] Q. Huang, Y. Qiu, W. Bao, M. A. Green, J. W. Lynn, Y. C. Gasparovic, T. Wu, G. Wu, and X. H. Chen, Phys. Rev. Lett. **101**, 257003 (2008).

[33] J. K. Dong, L. Ding, H. Wang, X. F. Wang, T. Wu, G. Wu, X. H. Chen, and S. Y. Li, New J. Phys. **10**, 123031 (2008).

[34] N. Ni, S. L. Bud'ko, A. Kreyssig, S. Nandi, G. E. Rustan, A. I. Goldman, S. Gupta, J. D. Corbett, A. Kracher, and P. C. Canfield, Phys. Rev. B **78**, 014507 (2008).

[35] B. Kolk, in *Dynamical Properties of Solids*, edited by G. K. Horton and A. A. Maradudin (North-Holland, Amsterdam, 1984), Vol. 5, p. 3.